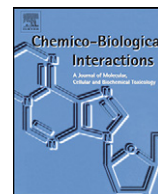




ELSEVIER

Contents lists available at ScienceDirect

## Chemico-Biological Interactions

journal homepage: [www.elsevier.com/locate/chembioint](http://www.elsevier.com/locate/chembioint)

## Anti-proliferative and pro-apoptotic effect of CPT13, a novel camptothecin analog, on human colon cancer HCT8 cell line

Li-Min Wang<sup>a,b</sup>, Qing-Yong Li<sup>a</sup>, Yuan-Gang Zu<sup>a,\*</sup>, Yu-Jie Fu<sup>a</sup>,  
Li-Yan Chen<sup>a</sup>, Hong-Yan Lv<sup>a</sup>, Li-Ping Yao<sup>a</sup>, Shou-Gang Jiang<sup>a</sup>

<sup>a</sup> Key Laboratory of Forest Plant Ecology, Northeast Forestry University, Ministry of Education, Harbin 150040, China

<sup>b</sup> College of Basic Medicine, Jiamusi University, Jiamusi 154007, China

## ARTICLE INFO

## Article history:

Received 8 May 2008

Received in revised form 14 July 2008

Accepted 17 July 2008

Available online 30 July 2008

## Keywords:

Camptothecin analog

HCT8

Proliferation

Apoptosis

## ABSTRACT

10-(2-Pyrazolyl-ethoxy)-(20S)-camptothecin (CPT13) is a novel semi-synthetic analogue of camptothecin, our previous report had shown that it possessed higher in vitro cytotoxicity activity towards human colon cancer HCT8 cell line than topotecan. In this study, the anti-proliferative effect of CPT13 on HCT8 cell line in vitro was analyzed. In order to further explore the underlying mechanism of cell growth inhibition of CPT13 towards HCT8 cell line, the cell cycle distribution, apoptosis proportion, the nuclei morphological changes and caspase-8 and caspase-3 activities were measured. Additionally the changes of mitochondrial morphology and membrane potential ( $\Delta\Psi_m$ ) were analyzed by atomic force microscopy (AFM) and flow cytometry, respectively. The results showed that CPT13 inhibited HCT8 cell growth by causing cell cycle arrest at G<sub>2</sub>/M transition and induced apoptosis, as evidenced by the typical apoptotic morphology such as condensation and fragmentation of nuclei and formation of apoptotic bodies. The changes of mitochondrial morphology, dose-dependently decrease in  $\Delta\Psi_m$  and the enhancement of caspase-8 and caspase-3 activities were observed in different concentrations of drug treatment group. Our results suggest that CPT13 induces apoptosis by alternations of mitochondrial transmembrane depolarization, activation of caspase-8 and caspase-3. Therefore, CPT13 appears to be a potent drug against human colon cancer via induction of apoptosis and may be used as an alternative drug to therapy cancer.

© 2008 Elsevier Ireland Ltd. All rights reserved.

### 1. Introduction

Camptothecin (CPT) is an alkaloid originally isolated from a native Chinese tree *Camptotheca acuminata* [1]. In the past several decades, CPT and its analogues, as a promising new class of anticancer drugs, have advanced to the forefront of several areas of therapeutic and developmental chemotherapy [2–4]. Interest for its clinic application as an anticancer agent declined due to its severe side effect, extremely poor water solubility and rapid inactivation through lactone ring hydrolysis at physiological pH. These

problems prompted the synthesis of many CPT derivatives, such as topotecan and irinotecan that have been approved for marketing as clinical anti-tumor agents [5,6]. More analogues are in various stages of clinical trials. It was reported that the designed camptothecin analogues would possess two criteria: improved water solubility; increased cytotoxicity. Recently, we have reported a new synthetic methodology to transform 10-hydroxy-camptothecin to camptothecin quaternary salts, which placed the several water-solubilizing groups in the 10-position of CPT. These salts showed good water solubility and different in vitro cytotoxicities [7]. In order to establish generality of this method, we also carried out this transformation with other heterocyclic aromatic compounds, and a series of camptothecin derivatives were prepared and preliminary

\* Corresponding author. Tel.: +86 451 82191517; fax: +86 451 82102082.  
E-mail address: [wlmton@163.com](mailto:wlmton@163.com) (Y.-G. Zu).

anti-tumor activity were evaluated, among them, 10-(2-pyrazolyl-ethoxy)-(20S)-camptothecin (CPT13) exhibited good anti-tumor activity in vitro, especially cytotoxicity towards human colon cancer HCT8 cell line was higher than that of topotecan [8]. The anti-proliferative activity and the mechanism of action of CPT13 against human colon cancer HCT8 cell line were not reported in previous study.

In the present study, anti-proliferative activity of CPT13 on HCT8 cell line was analyzed by MTT method. Moreover, the mechanism of action of CPT13 on HCT8 cell line was investigated by flow cytometry and atomic force microscopy (AFM).

## 2. Materials and methods

### 2.1. Chemicals and reagents

The compound CPT13 was synthesized as described previously [8], and the structure is shown in Fig. 1. The purity of this compound was assayed by HPLC, and the purity was 98.8%. 5-Diphenyltetrazolium bromide (MTT), Acridine Orange (AO), rhodamine123 (Rh123) were purchased from Sigma–Aldrich Inc. (St. Louis, MO).

### 2.2. Cell culture

The human colon cancer cell line HCT8 was obtained from Academy of Medicinal Sciences (China) and maintained in the RPMI-1640 (Hyclone, Logan, Utah, USA) with 10% fetal bovine serum (FBS, Tianjin Biotechnology Co. Ltd., China), 100 µg/ml streptomycin and 100 unit/ml penicillin at 37 °C in a 5% CO<sub>2</sub> atmosphere.

### 2.3. Cell proliferation assay

Cell proliferation was measured using MTT assay. HCT8 cells in exponentially growth phase were cultured at a density of  $1 \times 10^6$  cells/ml in a 96-well plate. After treatment with 0.008–25 µM CPT13 for 24, 48 and 72 h, MTT solution (5.0 mg/ml in phosphate-buffered saline) was added (10.0 µl/well), and the plates were incubated for another 4 h at 37 °C. The purple formazan crystals were dissolved in 100.0 µl DMSO per well. After 10 min, the plates were read on microplate reader (American Bio-Tek) at 570 nm. The cells without drugs were used as control. The survival

of the cells was expressed as percentage of untreated control wells. Assays were performed on three independent experiments.

### 2.4. Flow cytometric analysis of cell cycle and apoptosis

Briefly,  $1 \times 10^6$  cells/ml HCT8 cells were seeded in six-well plate and left for 24 h in incubator to resume exponential growth. Cells were exposed to drugs and incubated for 48 h. Then the cells were harvested and washed with PBS. After suspension in 800 µl PBS, 200 µl CyStain (Partec GmbH, Germany) was added for cell cycle experiments. The extent of apoptosis was measured through annexinV-FITC apoptosis detection kit (Beyotime Institute of Biotechnology, China) as described by the manufacture's instruction. After cells were exposed to drugs for 48 h, then they were collected and washed with PBS twice, gently resuspended in annexin-V binding buffer and incubated with annexinV-FITC/PI in dark for 15 min and analyzed by flow cytometry using cell quest software (BD Biosciences, USA). The fraction of cell population in different quadrants was analyzed using quadrant statistics. Cells in the lower left quadrant represented survivals, lower right quadrant represented apoptosis and in the upper right quadrant represented necrosis or post-apoptotic necrosis.

### 2.5. Morphological observation of nuclear change

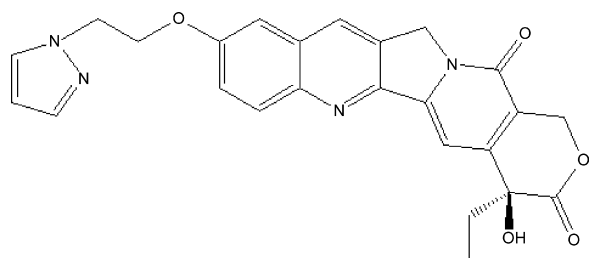
HCT8 cells ( $1 \times 10^6$  cells/ml) were seeded in 96-well plates and treated with 0.2 µM CPT13 for 48 h at 37 °C. Cells were collected, washed, fixed in 4% paraformaldehyde for 30 min and stained with 100 µg/ml AO for 5 min at room temperature, the apoptotic cells were visualized using inverted fluorescence microscope (Nikon TE2000, Tokyo, Japan).

### 2.6. The changes of mitochondrial membrane potential ( $\Delta\Psi_m$ )

The changes in  $\Delta\Psi_m$  were estimated using the fluorescent cationic dye rhodamine123 (Rh123) [9], which accumulates in mitochondria as a direct function of the membrane potential and is released upon membrane depolarization [10]. Briefly,  $1 \times 10^6$  cells/ml HCT8 cells were plated in a 6-well plate, exposed to different concentrations of CPT13 for 48 h, washed and finally harvested in chilled PBS containing Rh123. The samples were incubated at 37 °C for 30 min in dark, cells were then washed twice with PBS and analyzed immediately by flow cytometry.

### 2.7. Evaluation of morphological changes of mitochondria by atomic force microscopy (AFM)

Mitochondria were isolated from the HCT8 cells by mechanical lysis and differential centrifugation. Briefly, cells were washed with cold PBS at 4 °C and centrifuged at  $600 \times g$ /min. The pellet was resuspended in cold isolation buffer, and the cells were disrupted by homogenization.



10-(2-pyrazolyl-ethoxy)-(20s)-camptothecin (CPT13)

Fig. 1. Chemical structure of CPT13.

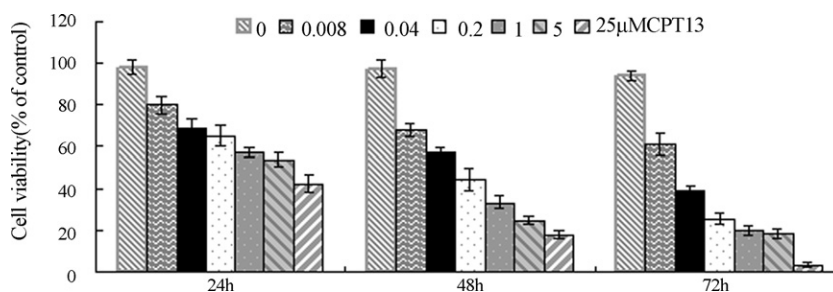


**Fig. 2.** Influence of CPT13 on proliferation of HCT8 cell line. HCT8 cells were treated with CPT13 for 24, 48 and 72 h at the indicated concentrations, and viability was measured by MTT assay. The values for each CPT13 concentration tested represent the average (mean  $\pm$  S.D.) from eight replicate wells and are representative of three separate experiments.

Nonlysed cells and nuclei were spun down by centrifugation at  $1000 \times g/\text{min}$  for 10 min. The supernatant was further centrifuged at  $3500 \times g/\text{min}$  for 10 min. The pellet, designated as the mitochondrial fraction, was suspended in deionized distilled water and dropped on fresh mica surface, then air-dried for AFM imaging. Imaging was performed with a commercial AFM system (Picoplus, Molecular Imaging, Tempe, USA).

## 2.8. Measurement of caspase-8 and caspase-3 activities

The activation of caspase-8 and caspase-3 were determined with the colorimetric kit (Nanjing kaiji Bio-Tek Corporation, China). HCT8 cells ( $1 \times 10^6$  cells/ml) were har-

vested and washed once with PBS. After the HCT8 cells were lysed, reaction buffer was added to the HCT8 cells followed by the additional  $5 \mu\text{l}$  of caspase-8 or caspase-3 colorimetric substrate (DEVD-pNA) and incubated in a 96-well plate for 4 h at  $37^\circ\text{C}$  in a  $\text{CO}_2$  incubator. The plate was then read with a microplate reader at 405 nm. Activities of caspase-8 and caspase-3 were expressed relative to the optical density value (OD).

## 2.9. Statistical analysis

Results are expressed as mean  $\pm$  S.D., The statistical evaluation of the results was performed by Student's *t*-test. Significance was established at  $p < 0.05$ .

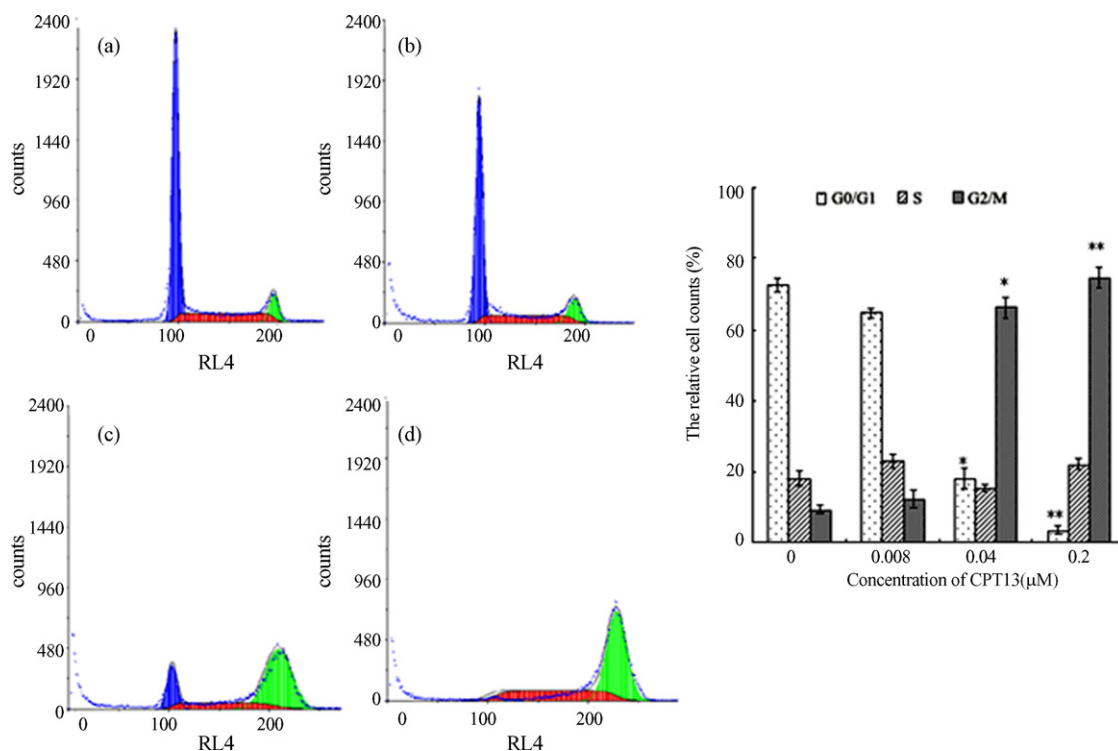


**Fig. 3.** Effect of CPT13 on the cell cycle distribution of HCT8 cells. (A) Flow cytometric analysis of HCT8 cell cycle distribution. The x-axis represents fluorescent intensity on a logarithmic scale, whereas the y-axis represents the number of events. (a) Control; (b) treatment with  $0.008 \mu\text{M}$  CPT13; (c) treatment with  $0.04 \mu\text{M}$  CPT13; (d) treatment with  $0.2 \mu\text{M}$  CPT13. (B) The results were analyzed by Mod Fit LT 3.0. Data are presented as mean  $\pm$  S.D. ( $n = 3$ ). \*\* $p < 0.01$ , \* $p < 0.05$ ;  $p$  value compared with the control group ( $0 \mu\text{M}$ ).

### 3. Results

#### 3.1. Anti-proliferative activity of CPT13

The growth of the HCT8 cells in the presence of various concentrations of CPT13 was examined. As shown in Fig. 2, under the experimental conditions (24, 48 and 72 h), CPT13 decreased HCT8 viable cell number in a time- and concentration-dependent manner (with increasing concentrations from 0.008 to 25  $\mu\text{M}$ ). HCT8 cells treated with 5 and 25  $\mu\text{M}$  CPT13 for 72 h induced 81.6% and 90.3% reductions in cell number, respectively.

#### 3.2. Flow cytometric analysis of HCT8 cell cycle distribution and apoptosis

The cell cycle distribution was analyzed by Multicycle software to investigate the effects of CPT13 on the cell cycle, as shown in Fig. 3, HCT8 cells were treated with different concentrations of CPT13 for 48 h. An accumulation of HCT8 cells in the  $G_2/M$  phases (from  $9.31 \pm 1.17\%$  to  $74.42 \pm 2.98\%$ ) was observed. Compared to the untreated group, a significant increase in percentage of cells in  $G_2/M$  phase was found after the cells treated with CPT13 at 0.2  $\mu\text{M}$  ( $p < 0.01$ ) (Fig. 3d). The apoptosis results showed that the

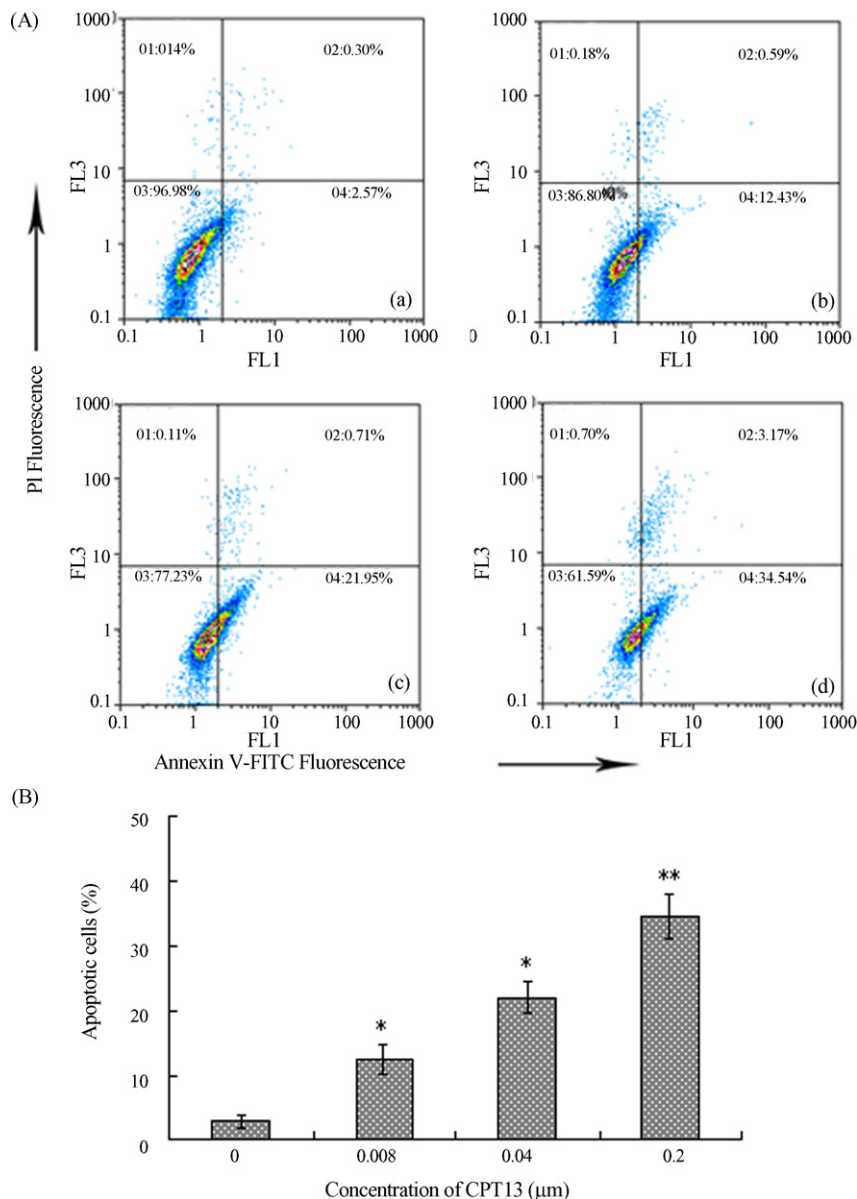


**Fig. 4.** Apoptotic population of HCT8 cells. (A) Flow cytometric analysis of CPT13-induced apoptosis in HCT8 cells using annexinV-FITC/PI. (a) Control; (b) treatment with 0.008  $\mu\text{M}$  CPT13; (c) treatment with 0.04  $\mu\text{M}$  CPT13; (d) treatment with 0.2  $\mu\text{M}$  CPT13. Quadrants: Q3: live cells; Q4: apoptotic cells; Q2: necrotic cells. (B) Columns, mean of three experiments, data are presented as mean  $\pm$  S.D. \*\* $p < 0.01$ , \* $p < 0.05$ ;  $p$  value compared with the control group (0  $\mu\text{M}$ ).

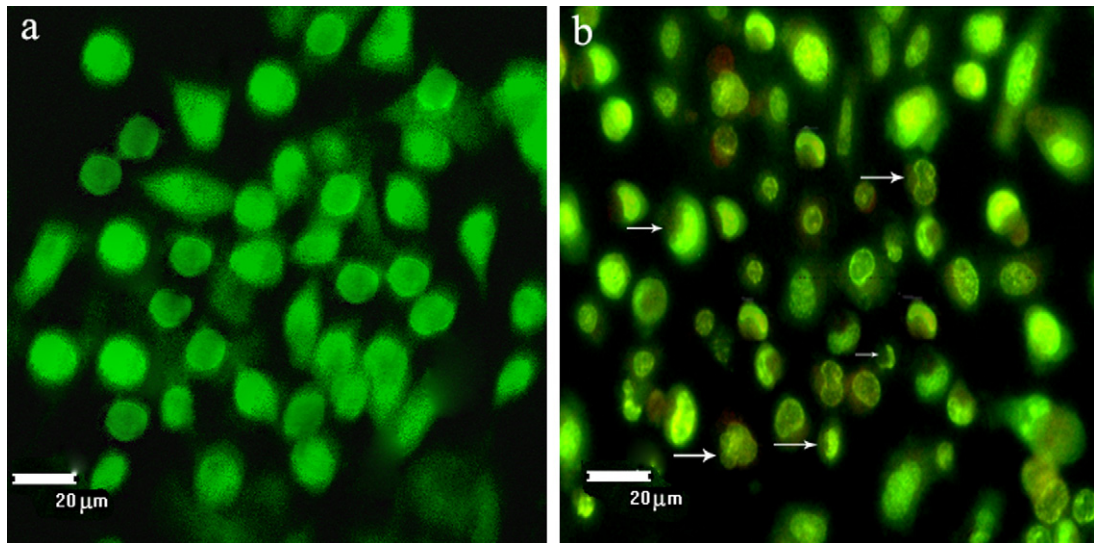


**Fig. 5.** Morphological observation of HCT8 cells treated with 0.2  $\mu\text{M}$  CPT13 for 48 h under inverted fluorescent microscope. Cells undergoing apoptosis and nuclear fragmentation are indicated by arrows. (a) Untreated cells; (b) treated with CPT13.

mean apoptotic population of normal HCT8 cells was  $2.57 \pm 1.12\%$ , however, the apoptotic population increased to  $34.54 \pm 3.38\%$  after the cells treatment with 0.2  $\mu\text{M}$  CPT13 for 48 h (Fig. 4). At the same time, the proportion of the cells in  $G_2/M$  phase increased obviously. Therefore, the anti-proliferative effect of CPT13 and cell apoptosis induction may be related to the accumulation of the cells in  $G_2/M$  phase.

### 3.3. Chromatin condensation and nuclear morphology changes

AO staining showed that there were significant morphological changes in the nuclear chromatin. In the untreated group, the nuclei were stained a less bright green and the color was homogeneous (Fig. 5a). After treating with 0.2  $\mu\text{M}$  CPT13 for 48 h, the yellow-green emission light in apoptotic cells was much brighter than the control cells. Nuclear of crescent-shaped or even strip-shaped debris and condensed chromatin could also be found in many treated cells, and some of them formed the structure of apoptotic bodies, which is one of the classic characteristics of apoptotic cells (Fig. 5b).

### 3.4. Loss of mitochondrial membrane potential of HCT8 cells induced by CPT13

To evaluate the role of mitochondria in CPT13-induced apoptosis, we investigated its ability to induce alterations in  $\Delta\Psi_m$ . Control HCT8 cells elicited maximal Rh123 fluorescence reflecting intact, functional mitochondria. Various concentrations of CPT13 treatment results in rapid dose-dependent dissipation of  $\Delta\Psi_m$  as detected by consequent decrease in mean fluorescence. Significant decrease in  $\Delta\Psi_m$  starts at 0.04  $\mu\text{M}$  CPT13 ( $p < 0.05$ ). These data showed that CPT13 induces apoptosis accompanied by the alterations in the mitochondrial membrane potential (Fig. 6).

### 3.5. Analysis of atomic force microscopy (AFM) images

To assess the apoptosis effect induced by CPT13 in HCT8 cells, the morphological changes of mitochondria were observed by AFM. As can be seen from Fig. 7, after the cells treated with 0.2  $\mu\text{M}$  CPT13 for 48 h, the surface of mitochondrial membranes changed distinctly compared to those untreated cells. The surface of CPT13 group became rougher than that of untreated group. The surface of normal mitochondria was smooth and integrity (Fig. 7a and b), after exposed to CPT13, some debris could be observed around the apical end of the mitochondrial membrane and the outer membrane collapsed, inner membrane dividing a mitochondrion into several compartments (Fig. 7c and d). It is postulated that the debris originates from the residual cristae.

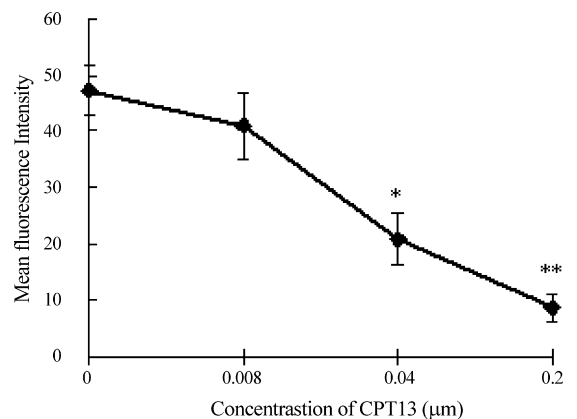


**Fig. 6.** The changes of the mitochondrial membrane potential of HCT8 cells induced by CPT13. Results are mean  $\pm$  S.D. of three independent experiments.



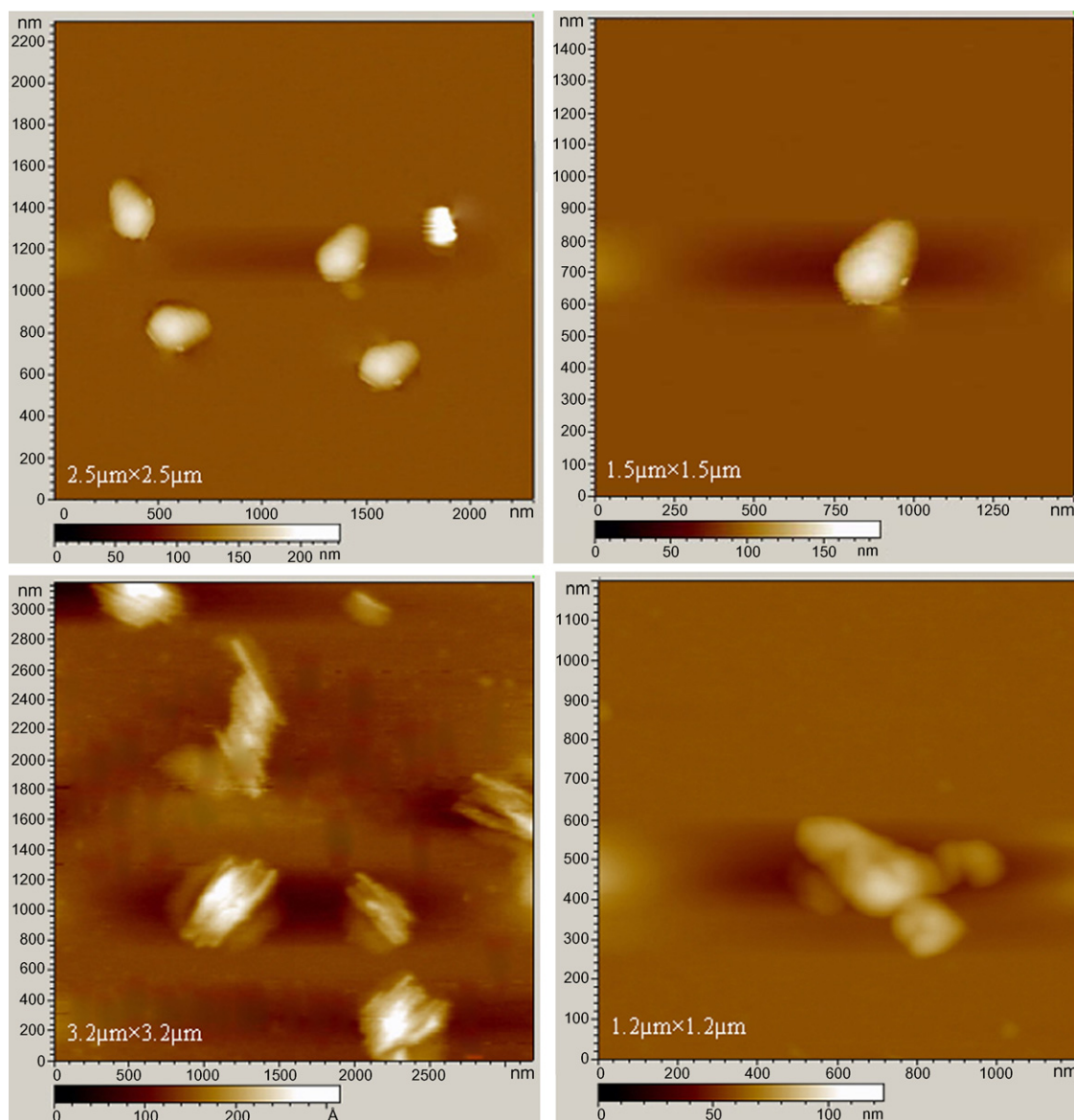


Fig. 7. AFM images of mitochondrion of HCT8. (a and b) Untreated with CPT13; (c and d) treated with 0.2  $\mu\text{M}$  CPT13 for 48 h.

### 3.6. Effect of CPT13 on caspase-8 and caspase-3 activities

The changes of caspase-8 and caspase-3 activities in HCT8 cells treated with CPT13 were detected by colorimetric systemic assays. The dose-dependent elevation of caspase-8 and caspase-3 activities was observed in drug treatment group. The most obvious changes were observed in the cells treated with 0.2  $\mu\text{M}$  CPT13 for 48 h, the OD values were reached to  $0.235 \pm 0.021$  and  $0.214 \pm 0.017$ , respectively, it was significant in comparison to the control group ( $p < 0.01$ , see Fig. 8).

## 4. Discussion

Colonic cancer is one of the most common malignant tumors in some areas of the world. Despite many advances

in the field of cancer therapeutics, colonic cancer continues to be a main cause of death, which is in part due to the failure of chemotherapy [11]. Therefore, searching for new anti-tumor and other medical substances and studying their medical value have become a matter of great significance. Anticancer drug are usually designed as having low side effects and target-specific anti-proliferative activity to the cancer cells [12], keeping this in mind we investigated the anti-proliferative activity of CPT13 against HCT8 cells, as a result, CPT13 exhibited good anti-proliferative activity against HCT8 cell line.

Induction of cell apoptosis is a useful approach in cancer therapies [13,14]. Apoptosis is a physiological process that functions as an essential mechanism of tissue homeostasis and is regarded as the preferred way to eliminate unwanted cells [15,16]. Cancer is caused by the disruption

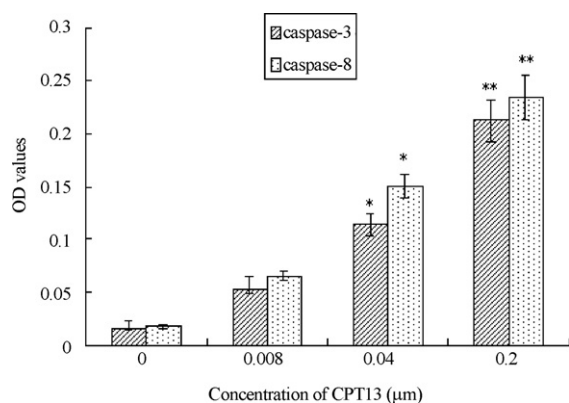


**Fig. 8.** Effect of CPT13 on caspase-8 and caspase-3 activities. Data are presented as mean  $\pm$  S.D. ( $n=3$ ). \*\* $p < 0.01$ , \* $p < 0.05$ ,  $p$  value compared with the control group (0  $\mu$ M).

of cellular homeostasis between cell death and cell proliferation, so that compounds which can induce apoptosis are considered to have potential as anticancer agents [17,18].

Apoptosis is characterized by a series of stereotypic morphological changes such as formation of apoptotic bodies, nuclear and cytoplasmic condensation, chromatin fragmentation, shrinkage of cells and bleb formation. Apoptotic is linked to cell cycle arrest. The cell cycle is a complex process by which cells receive different growth controlling signals that are integrated and processed at various points known as checkpoints [19]. The cell growth is controlled when cells are not allowed to proceed further at these checkpoints, and defects in normal regulation lead to excessive proliferation of genetically damaged cells, which eventually results in the formation of cancerous lesions. Blockade of the cell cycle is regarded as an effective strategy in the development of cancer therapies [20,21]. Our data showed that CPT13 can induce apoptosis in HCT8 cells, which is related to the accumulation of the  $G_2/M$  phase cells.

Mitochondria play a central role in the regulation of apoptotic signaling [22,23]. Disruption of the mitochondrial membrane potential is one of the earliest intracellular events that occur following induction of apoptosis [24]. Since the  $\Delta\Psi_m$  decrease was concentration dependent in the HCT8 cells treated with CPT13, we presumed that  $\Delta\Psi_m$  decrease may be one of the main pathways in apoptotic process of CPT13 induced cell death. Due to mitochondrial outer membrane changes are important features of cell apoptosis [25]. Imaging of the outer contours of the mitochondrial membrane was analyzed using atomic force microscopy, which was first applied for analysing mitochondrial morphological changes. The AFM results support a role of mitochondria pathway in apoptosis induced by CPT13.

Caspases, the cytoplasmic aspartate-specific cysteine proteases, play an important role in apoptosis [26,27]. It is demonstrated that caspases can disrupt mitochondrial function during apoptosis [28], therefore caspase-8 and caspase-3 activities were detected by caspases colorimetric assay. The study shows that CPT13 can activate caspase-8, and then caspase-8 can activate caspase-3, which in turn

may cleave cytoskeletal and nuclear proteins, disrupt mitochondrial function and finally induce apoptosis.

## 5. Conclusions

Our current study demonstrates that CPT13, a camptothecin analog, promoted cell apoptosis and inhibited cell growth in human colonic cancer cell line HCT8. Like camptothecin [29], CPT13-induced cell apoptosis and growth inhibition may involve cell cycle arrest and the activation of mitochondrial apoptotic pathway. CPT13 might produce these effects through numerous mechanisms at different levels. Although many details of the effects of CPT13 are still poorly understood, the in vitro findings in the present study offer a significant groundwork for future essential in vitro and in vivo study and clinical application.

## Acknowledgements

The authors gratefully acknowledge the financial support by National Natural Science Foundation of China (30600052), Program for New Century Excellent Talents in University (NCET-06-0329), Program of Science and Technology from State Forestry Administration (2007–2012).

## References

- [1] C.F. Verschraegen, K. Jaeckle, B. Giovannella, Alternative administration of camptothecin analogues, *Ann. N. Y. Acad. Sci.* 922 (2000) 237–246.
- [2] J. Dancy, E.A. Eisenhauer, Current perspectives on camptothecin in cancer treatment, *Br. J. Cancer* 74 (1996) 327–338.
- [3] L. Bomgaars, S.L. Berg, S.M. Blaney, The development of camptothecin analogs in childhood cancers, *Oncologist* 6 (2001) 506–516.
- [4] Q.Y. Li, Y.G. Zu, R.Z. Shi, L.P. Yao, Review camptothecin: current perspectives, *Curr. Med. Chem.* 13 (2006) 2021–2039.
- [5] C.H. Takimoto, J. Wright, S.G. Arbuck, Clinical applications of the camptothecins, *Biochim. Biophys. Acta* 1400 (1998) 107–119.
- [6] J.F. Pizzolato, L.B. Saltz, The camptothecins, *Lancet* 361 (2003) 2235–2242.
- [7] Y.G. Zu, Q.Y. Li, Y.J. Fu, Synthesis and cytotoxicity of water soluble quaternary salt derivatives of camptothecin, *Bioorg. Med. Chem. Lett.* 14 (2004) 4023–4026.
- [8] Q.Y. Li, Y.G. Zu, R.Z. Shi, Synthesis and antitumor activity of novel 10-substituted camptothecin analogues, *Bioorg. Med. Chem.* 14 (2006) 7175–7182.
- [9] N. Zamzami, C. Maise, D. Metivier, G. Kroemer, Measurement of membrane permeability and permeability transition of mitochondria, *Methods Cell Biol.* 65 (2001) 147–158.
- [10] C.M. Palmeira, A.J.M. Moreno, V.M.C. Madeira, K.B. Wallace, Continuous monitoring of mitochondrial membrane potential in hepatocyte cell suspensions, *J. Pharmacol. Toxicol. Methods* 35 (1996) 35–43.
- [11] M.V. Grau, J.R. Rees, J.A. Baron, Chemoprevention in gastrointestinal cancers: current status, *Basic Clin. Pharmacol. Toxicol.* 98 (2006) 281–287.
- [12] M.V. Blagosklonny, A.B. Pardee, Exploiting cancer cell cycling for selective protection of normal cells, *Cancer Res.* 61 (2002) 4301–4305.
- [13] B. Zhivotovsky, G. Kroemer, Apoptosis and genomic instability, *Nat. Rev. Mol. Cell Biol.* 9 (2004) 752–762.
- [14] N.N. Danial, S.J. Korsmeyer, Cell death: critical control points, *Cell* 116 (2004) 205–219.
- [15] S. Elmore, Apoptosis: a review of programmed cell death, *Toxicol. Pathol.* 35 (2007) 495–516.
- [16] K. Vermeulen, D.R. Van Bockstaele, Z.N. Berneman, Apoptosis: mechanisms and relevance in cancer, *Ann. Hematol.* 84 (2005) 627–639.
- [17] C.B. Thompson, Apoptosis in the pathogenesis and treatment of disease, *Science* 267 (1995) 1456–1462.
- [18] O.S. Frankfurt, A. Krishan, Apoptosis-based drug screening and detection of selective toxicity to cancer cells, *Anticancer Drugs* 14 (2003) 555–561.

- [19] M.B. Kastan, J. Bartek, Cell-cycle checkpoints and cancer, *Nature* 432 (2004) 316–323.
- [20] J.K. Buolamwini, Cell cycle molecular targets in novel anticancer drug discovery, *Curr. Pharm. Des.* 6 (2000) 379–392.
- [21] E.R. McDonald, W.S. El-Deiry, Cell cycle control as a basis for cancer drug development, *Int. J. Oncol.* 16 (2000) 871–886.
- [22] V. Gogvadze, S. Orrenius, Mitochondrial regulation of apoptotic cell death, *Chem. Biol. Interact.* 163 (2006) 4–14.
- [23] D.R. Green, Apoptotic pathways: the roads to run, *Cell* 94 (1998) 695–698.
- [24] J. Han, L.A. Goldstein, B.R. Gastman, H. Rabinowich, Interrelated roles for Mcl-1 and BIM in regulation of TRAIL-mediated mitochondrial apoptosis, *J. Biol. Chem.* 281 (2006) 10153–10163.
- [25] A. Sessa, M.M. Marques, M.M. Monteiro, Morphology of mitochondrial permeability transition: morphometric volumetry in apoptotic cells, *Anat. Rec. A: Discov. Mol. Cell Evol. Biol.* 281 (2004) 1337–1351.
- [26] N.A. Thornberry, Caspases: key mediators of apoptosis, *Chem. Biol.* 5 (1998) R97–R103.
- [27] J.E. Chipuk, D.R. Green, Do inducers of apoptosis triggers caspase independent cell death? *Nat. Rev. Mol. Cell Biol.* 6 (2005) 268–275.
- [28] J.E. Ricci, R.A. Gottlieb, D.R. Green, Caspase-mediated loss of mitochondrial function and generation of reactive oxygen species during apoptosis, *J. Cell Biol.* 160 (2003) 65–75.
- [29] N. Johnson, T.T. Ng, J.M. Parkin, Camptothecin causes cell cycle perturbations within T-lymphoblastoid cells followed by dose dependent induction of apoptosis, *Leuk. Res.* 21 (1997) 961–972.